

## IMPLICATIONS OF THE IRAS DATA FOR GALACTIC GAMMA-RAY ASTRONOMY AND EGRET

F. W. STECKER

Lab. for High Energy Astrophysics, NASA Goddard Space Flight Center  
Greenbelt, Maryland 20771, U.S.A.

## ABSTRACT

Using the results of  $\gamma$ -ray, millimeter wave and far infrared surveys of the galaxy, one can derive a logically consistent picture of the large scale distribution of galactic gas and cosmic rays, one tied to the overall processes of stellar birth and destruction on a galactic scale. Using the results of the IRAS far-infrared survey of the galaxy, we have obtained the large scale radial distributions of galactic far-infrared emission independently for both the northern and southern hemisphere sides of the Galaxy. We find the dominant feature in these distributions to be a broad peak coincident with the "5 kpc" molecular gas cloud ring. We also find evidence of spiral arm features. Strong correlations are evident between the large scale galactic distributions of far infrared emission,  $\gamma$ -ray emission and total CO emission. There is a particularly tight correlation between the distribution of warm molecular clouds and far-infrared emission on a galactic scale. The 5 kpc ring has been evident in existing galactic  $\gamma$ -ray data. The extent to which the more detailed spiral arm features are evident in the more resolved EGRET data will help to determine more precisely the propagation characteristics of galactic cosmic rays.

## I. INTRODUCTION

Using observational and theoretical arguments from other branches of astronomy, Stecker (1969) pointed out that the most likely explanation for the  $\gamma$ -ray flux from the inner plane of the Galaxy observed by the pioneering OSO-3 satellite experiment (Clark, et al. 1968) was the existence of a significant component of interstellar molecular hydrogen gas in cool dense clouds. More recent satellite observations imply that  $\gamma$ -ray emission is highly non-uniform in the Galaxy, and that its emissivity distribution peaks about halfway between the sun and the galactic center. The  $\gamma$ -ray emissivity distribution bears a strong resemblance to the distribution of molecular clouds in the Galaxy. This similarity, coupled with the lack of enough gas in atomic form (HI) to explain the  $\gamma$ -ray measurements, led to the supposition that  $H_2$  is far more abundant in the inner Galaxy than HI, and that  $H_2$  plays the major role in producing galactic  $\gamma$ -rays (Stecker, et al. 1975). The  $H_2$  hypothesis was proven by observation five years later with the discovery of a large, roughly ring-shaped distribution of molecular clouds in the inner galaxy (Scoville and Solomon 1975). A detailed survey of most of the galactic plane was made from the SAS-2 satellite detector (Fichtel, et al. 1975). The proof of the correlation of galactic  $\gamma$ -ray emissivity (deduced from the SAS-2 data) with the molecular cloud component in the inner galaxy followed quickly (Solomon and Stecker 1974; Stecker, et al. 1975). Further analysis indicated that the cosmic-ray distribution in the inner galaxy is similar to that of supernova remnants and pulsars, supporting the hypothesis that most cosmic-rays are galactic in origin (Stecker 1975; Stecker 1976; Stecker and Jones 1977). Harding and Stecker (1985) (hereafter designated HS) performed a joint analysis of the SAS-2 and COS-B data, supporting the earlier conclusion of a galactic radial cosmic-ray gradient and the galactic origin hypothesis. By

taking a "synoptic" approach to galactic astronomy (Stecker 1981), using mm-wave and far-infrared galactic surveys and studies of other galaxies in conjunction with the galactic  $\gamma$ -ray surveys, one can relate galactic  $\gamma$ -ray production to the birth and death of young Population I stars in the Galaxy (Stecker 1976). As a new consideration here, we will present a detailed unfolding of the 100  $\mu$ m IRAS survey of the Galaxy and show how it sheds light on the meaning of past and future  $\gamma$ -ray surveys.

## .II. GALACTIC GAMMA-RAY PRODUCTION

Gamma-rays are produced in the Galaxy primarily by the electromagnetic processes of bremsstrahlung and Compton interactions of cosmic-ray electrons with interstellar gas and radiation fields respectively and by the strong interactions of cosmic-ray nuclei with interstellar gas, resulting in the production and almost immediate decay of neutral pions (Stecker 1971).

The pion decay  $\gamma$ -ray component can be calculated from the expression

$$q_{\pi}(E_{\gamma}) = 8\pi n_H \mu \int_{E_{th}}^{\infty} dE_p I(E_p) \int_{\lambda(E_{\gamma})}^{\infty} dE (E^2 - m_{\pi}^2)^{-1/2} \zeta_{\pi}(E_p) \sigma_{\pi}(E_{\pi}; E_p) \quad (1)$$

where  $\lambda(E_{\gamma}) = E_{\gamma} + (m_{\pi}^2/4E_{\gamma})$ ,  $\zeta_{\pi}$  is the neutral pion multiplicity, and  $\mu$  is a multiplicative enhancement factor which takes account of  $\alpha p$ ,  $p$ -He and  $\alpha$ -He interactions as well as  $pp$  interactions. This formula is derived in detail by Stecker (1971).

The calculation of this component hinges on the development of a model for the pion production function  $\sigma(E; E_p)$  which adequately describes the cross section and energy distribution of neutral pions produced in  $pp$  interactions at a given energy  $E_p$  as determined by accelerator data. The first such model, the "isobar-plus-fireball model", was developed by Stecker (1970) who noted the importance of nucleon isobar channels at the primary energies where most of the pions are produced. An update utilizing Feynman scaling for  $E_p > 5$  GeV, the "isobar-plus-scaling" model, was introduced by Stecker (1979) to calculate both the  $\gamma$ -ray and neutrino production spectra from pion decay, with emphasis on a discussion of the high energy neutrinos. Dermer (1986) has shown that such models which include isobar production provide an excellent fit to the accelerator data on pion production.

The differential  $\gamma$ -ray spectra from the various interactions discussed above are shown in Fig. 1 and the production rates for energies above 100 MeV are shown in Table 1 (Stecker 1989). The exact numbers given in Fig. 1 and Table 1 are not as significant as their relative rank of importance. It is clear that pion decay and bremsstrahlung are by far the most important production mechanisms, with their relative importance being energy dependent. As shown in Fig. 1, in the  $\gamma$ -ray energy range above 100 MeV, it is expected that  $\pi^0$  decay  $\gamma$ -rays dominate over bremsstrahlung  $\gamma$ -rays in the Galaxy. The reverse is true for lower-energy  $\gamma$ -rays since the  $\pi^0$  decay spectrum turns over at  $\sim 70$  MeV.

TABLE I  
LOCAL GALACTIC  $\gamma$ -RAY PRODUCTION RATES (STECKER 1989)

Process	$q(>0.1 \text{ GeV}) \text{ (cm}^{-3}\text{s}^{-1}\text{)}$	Fraction of Total
Pion Decay	$1.51 \times 10^{-25}$	66%
Bremsstrahlung	$6 \times 10^{-26}$	26%
Compton:		
Blackbody	$6 \times 10^{-27}$	
Far Infrared	$3 \times 10^{-27}$	5%
Starlight	$2 \times 10^{-27}$	
Total	$1.1 \times 10^{-26}$	
Pulsar Contribution	$6 \times 10^{-27}$	3%
Total Rate	$2.3 \times 10^{-25}$	

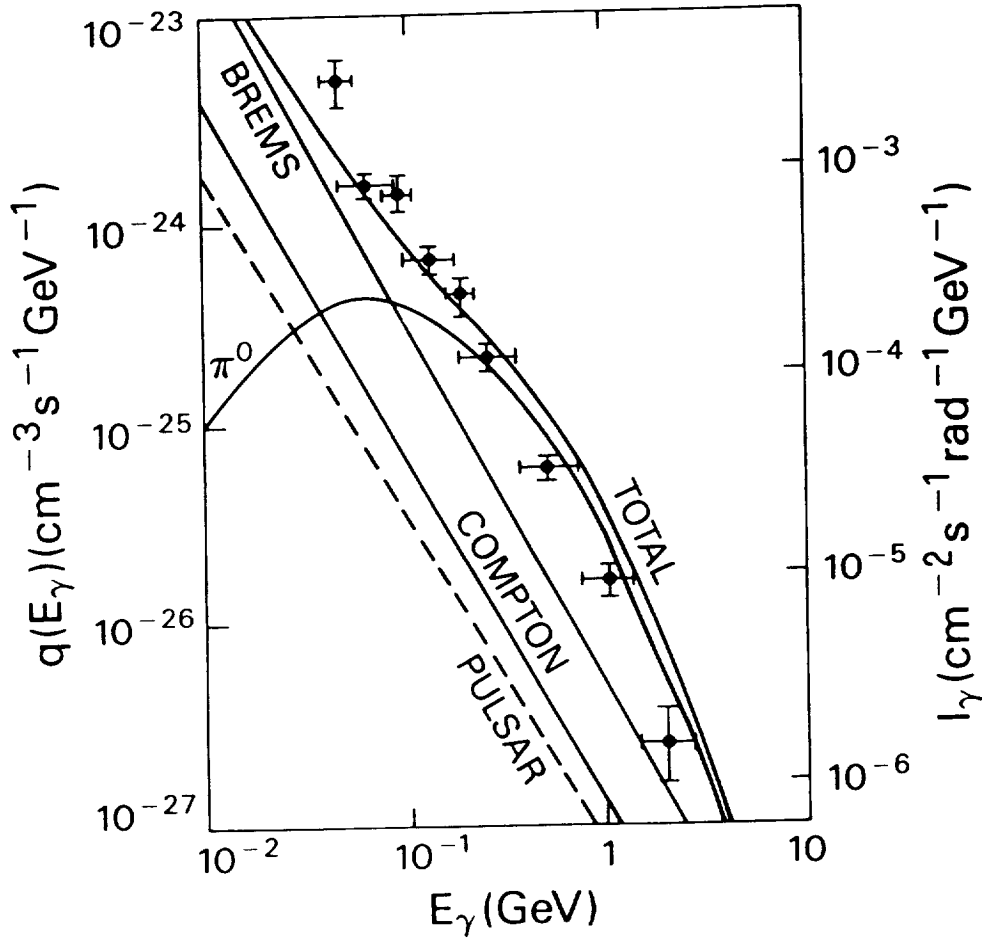


Fig 1. Local differential production spectra for major diffuse production processes and the pulsar component (left hand scale). The right hand flux scale and data points are from COS-B and SAS-2 inner Galaxy data.

### III. MM-WAVE CO SURVEYS

The vast bulk of the interstellar gas is in the form of hydrogen. Hydrogen in atomic form can be mapped by radio telescopes because of its spectral line at 21cm wavelength. However, hydrogen in molecular form does not emit such radio waves; the strongest spectral features from the  $H_2$  molecule are at ultraviolet wavelengths, not useful for large scale galactic structure studies. This radiation can only travel a mere kpc or so, before being absorbed by the interstellar dust.

Since the  $H_2$  molecule is the most stable form of hydrogen at low temperature, and since it is expected to be the predominant form of hydrogen in cool dense clouds, it is important to determine the abundance and distribution of  $H_2$  on a galactic scale. Radio emission from other molecules coexisting with  $H_2$  in cool interstellar molecular gas clouds can be used to trace  $H_2$  in the Galaxy. Because of its relative abundance as compared with other interstellar molecules (excluding  $H_2$ ), the CO molecule has become a useful  $H_2$  cloud tracer. This molecule has a radio spectral line at 2.64mm. The results of extensive galactic CO surveys have been published (Sanders, et al. 1986, Clemens, et al. 1986, Dame, et al. 1987, Bronfman, et al. 1988). These surveys, together with previous CO surveys have firmly established that the galactic distribution of  $H_2$  clouds is dramatically different from that of the more uniformly distributed atomic hydrogen. The atomic hydrogen gas density is relatively constant on a large scale in regions of the Galaxy between 4 and 15 kpc galactocentric radius, falling off inside of 4 kpc and outside of 15 kpc. In contrast, the  $H_2$  clouds have an entirely different distribution. They also fall off inside of 4 kpc (with the exception of a small nuclear region within 200 pc of the galactic center). However, the  $H_2$  clouds are strongly concentrated in an annular region or ring, reaching a peak density at a radial distance of ~5 kpc (Scoville and Solomon 1975), the same place where the  $\gamma$ -ray emission peaks (Solomon and Stecker 1974) and become almost non-existent outside of 10 kpc from the galactic center. Observations of the molecular cloud distribution in other spiral galaxies have revealed that some of these galaxies also have a ring-shaped distribution of molecular clouds (Young and Scoville 1982; Myers and Scoville 1987).

### IV. COSMIC RAYS IN THE INNER GALAXY

As discussed above, radio 2.6 mm-wave surveys of the Galaxy indicate that the average density of  $H_2$  is  $\sim 2 \text{ mol cm}^{-3}$  in the molecular cloud ring at a galactocentric distance of ~5 kpc, the "Great Galactic Ring", and drops off dramatically at <4 kpc and in the outer Galaxy. In the solar galactic neighborhood, most of the interstellar gas is probably HI. The increase in interstellar gas in the inner galaxy alone is not sufficient to explain the increased  $\gamma$ -ray emission there as deduced from the galactic  $\gamma$ -ray surveys. An accompanying increase in the cosmic ray intensity in the Great Galactic Ring is also called for. A deduction of the implied cosmic-ray distribution from the  $\gamma$ -ray observations shows that the cosmic rays increase (relative to the local intensity) by a factor of ~ 2-3 at a maximum coincident with the maximum in the gas density, in the 5 kpc region (Stecker 1976; Harding and Stecker 1985). This phenomenon is usually referred to as the galactic cosmic-ray gradient. The cosmic-ray distribution deduced using the  $\gamma$ -ray observations in conjunction with the deduced variation of total gas ( $HI+H_2$ ) in the Galaxy is, within experimental error, identical to the distribution of supernova

remnants and pulsars (Stecker 1975; Stecker and Jones 1977). This result is prima facie evidence that the bulk of the cosmic radiation originates either in galactic supernova explosions or the resulting pulsars. The striking resemblance between the distribution of cosmic rays implied by the existing  $\gamma$ -ray data and the distribution of supernova remnants and pulsars found by galactic radio surveys thus supports the hypothesis that most observed cosmic rays are born in our own Galaxy.

HS derived the radial distribution of  $\gamma$ -ray emission in the Galaxy from flux longitude profiles by geometrical unfolding techniques (e.g., Puget and Stecker 1974). Using both the final SAS-2 results and the COS-B results, they analyzed the northern and southern galactic regions separately. HS then made use of CO surveys of the southern hemisphere (Sanders, et al. 1984; Robinson, et al. 1984) in conjunction with the northern hemisphere CO data, to derive the radial distribution of cosmic rays on both sides of the galactic plane. They found that, in addition to the "5 kpc ring" of enhanced emission, there is evidence from the asymmetry in the radial distributions for spiral features which are consistent with those derived from the distribution of bright HII regions. They also found positive evidence for an increase in the cosmic ray flux in the inner Galaxy, particularly in the 4-5 kpc region, in both halves of the plane.

HS found general agreement in the shapes of the COS-B and SAS-2 emissivity distributions, the dominant features being a peak between 4 and 5 kpc in the North and a peak near 4 kpc in the South (taking the distance between the Sun and the Galactic Center to be 8.5 kpc). This seems to describe an asymmetric ring of emission. This emission region, which is a more large scale feature than an individual spiral arm, I will refer to as the "Great Galactic Ring". There is also a secondary peak of emission at ~6 kpc galactocentric radius in the South, which is more pronounced in the COS-B data. This feature, first pointed out by Stecker (1977), can be associated with the tangential direction to a spiral arm at  $\sim 310^\circ$ , referred to either as the Crux arm or an extension of the Sagittarius arm. HS presented a crude map of the Galaxy at  $\gamma$ -ray wavelengths. Their map resembles the more precise CO cloud map obtained from the Massachusetts-Stony Brook survey by Clemens, et al. (1988), also showing the "Great Galactic Ring".

Information on the distribution of gas in the Galaxy can be used in conjunction with the observed  $\gamma$ -ray emissivity to yield information on the galactic cosmic-ray distribution. The cosmic-ray density is proportional to  $q_\gamma$ , the  $\gamma$ -ray emissivity per H-atom, as derived from the observed  $\gamma$ -ray volume emissivity, total gas density,  $n_{TOT}$ , and gas scale height. The total gas density is the sum of molecular,  $n_{H_2}$ , and atomic,  $n_{HI}$ , densities,  $n_{TOT} = 2 n_{H_2} + n_{HI}$ .  $H_2$  densities were derived from galactic CO surveys. Longitude velocity data from these surveys can be analysed using a galactic rotation curve to give CO radial emissivity distributions, which can then be converted to  $H_2$  densities.

Figure 2 shows the radial distribution of  $q_\gamma (> 100 \text{ MeV})$  derived by HS. If all of the  $\gamma$ -ray emission were from diffuse processes, then  $q_\gamma$  would be proportional to the density of cosmic rays. The emissivity per H-atom derived from both the SAS-2 and COS-B data show evidence for an increase in the inner Galaxy in both the north and the south. The difference in the results may be partly due to uncertain subtractions for intrinsic background in the COS-B

detector (see discussion in HS and Stecker 1989).

Stecker and Jones (1977) investigated the effect of diffusion halo models on the galactocentric radial distribution of cosmic rays and made  $\gamma$ -ray emissivity fits to the SAS-2 data using a SN-pulsar source distribution for thin and thick (10 kpc) halos respectively. They showed that a large (10 kpc or more) diffusion halo can flatten the cosmic-ray gradient in the outer galaxy (see Fig. 3). However, the determination of a cosmic-ray gradient in the outer galaxy is quite difficult because of the uncertainty in separating distances along the line of sight without the type of rotational velocity information available to radio astronomers. Strong, et al. (1987) and Mayer, et al. (1987) find some hint of a cosmic-ray gradient in the outer Galaxy.

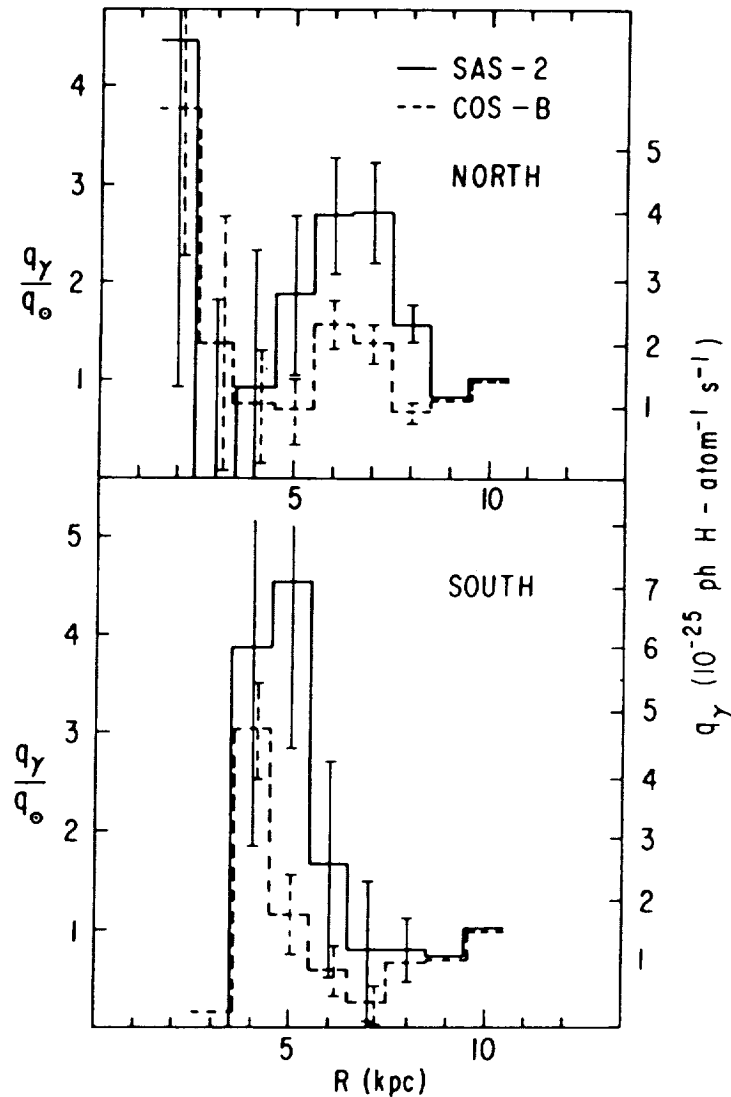


Fig. 2. Cosmic-ray distribution in the galactic plane obtained by Harding and Stecker (1985) from unfoldings of the SAS-2 and COS-B data.

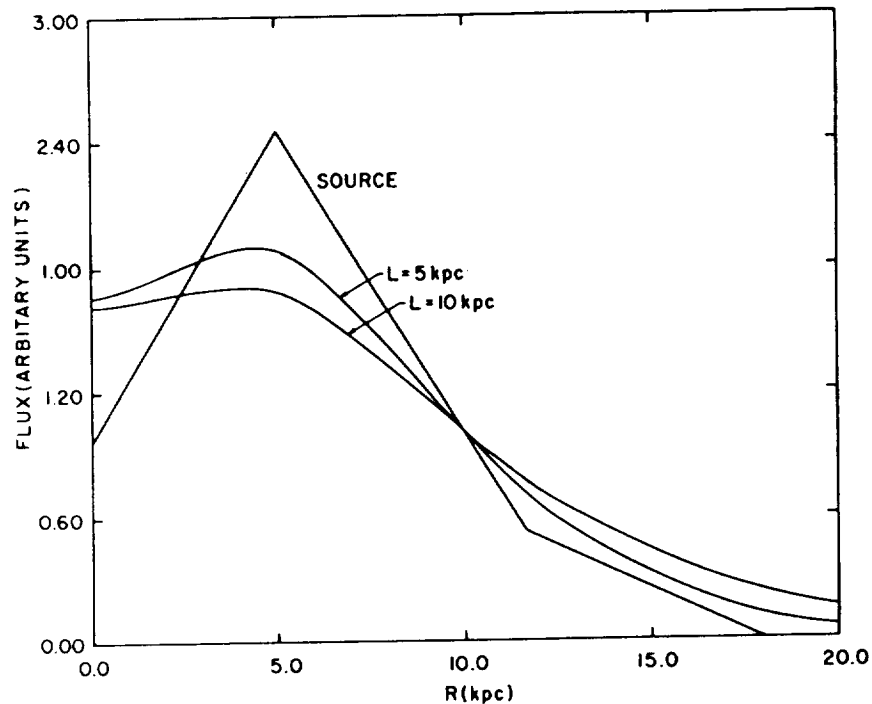


Fig. 3. Galactic radial distributions of cosmic-ray intensity using a weighted pulsar source model with a negligible diffusion halo and using diffusion halo models of thickness 5 and 10 kpc (Stecker and Jones 1977)

## VII. OTHER SURVEYS OF THE GALAXY AND THEIR IMPLICATIONS

Other Population I phenomena track with the radial distribution of CO, exhibiting the 5-kpc maximum. The pulsar and  $\gamma$ -ray distributions are remarkably similar (Harding and Stecker 1981). The distribution of HII regions and ionized gas (Lockman 1976) also falls into this category as does the distribution of far infrared emissivity (see below). All of these data lend support to the idea that the  $H_2$  cloud component of the interstellar medium plays the active dynamical role in Population I star formation processes which result in the observable structural characteristics of spiral galaxies (Burton 1976, Stecker 1976). The far infrared emission is from reradiation by dust of energy released primarily in the UV range by O, B and A stars.

Fazio and Stecker (1976) predicted that the galactic far infrared (FIR) distribution should also exhibit a strong correlation with the CO distribution and should have a pronounced peak at  $\sim 5$  kpc. This has indeed proved to be the case. Their basic hypothesis was that the bulk of the FIR radiation was the emission of dust heated by radiation from young Population I stars located

near molecular cloud complexes. In a detailed study of local complexes of giant molecular clouds, OB associations and HII regions using IRAS data, Leisawitz (1987) has shown that about 50-80% of the total luminosity is associated with molecular clouds seen in CO emission, 10-25% is associated with the HII regions, and the remainder surrounding the complex.

### VIII. ANALYSIS OF THE IRAS SURVEY OF THE GALAXY

The IRAS survey provides the first unobscured view of the IR distribution over the entire galactic disk. However, in determining the galactic distribution of IR emissivity, we do not have the additional information provided by velocity data, as one has in the case of radio line surveys. In the use of the essentially one dimensional galactic longitude flux distribution to obtain a galactocentric radial distribution of emission, one finds a commonality with the analysis of galactic  $\gamma$ -ray data, for which geometrical unfolding techniques have been developed (Puget and Stecker 1974; HS). A group of us (Stecker, et al., 1989) has been using these techniques on the IRAS data. We present here our first results. We will restrict ourselves to a presentation and discussion only of the 100  $\mu$ m infrared emission outside of 0.3 of the Sun-Galactic Center distance from the Galactic Center, excluding the strong source of emission in the very central region of the Galaxy. An extensive and quantitative report of all of our results, including other IRAS wavelength channels as well as a treatment of the inner 3 kpc of the Galaxy will be presented elsewhere.

We assumed cylindrical symmetry in each half of the galactic plane separately, so that the infrared emissivity derived in each half-plane would be a function of galactocentric radius  $R$ , independent of the height above the galactic plane up to a characteristic height  $h$ . Denoting  $r \equiv R/R_0$ , where the solar galactic radius  $R_0$  is presently defined to be 8.5 kpc, the flux as a function of longitude is given by

$$I(\ell) = R_0/2\pi \int_0^{b_m} db \int_0^{(h/R_0)\cot b} \epsilon(r) d\rho \quad (2)$$

where  $b$  is galactic latitude,  $\epsilon$  is emissivity per unit volume and  $\rho$  is line-of-sight distance in solar galactic radial units. If we divide the flux into inner and outer Galaxy contributions, assuming the outer Galaxy emissivity to be a constant out to some maximum radius  $R_m$ , the inner Galaxy emissivity can be unfolded using Laplace transforms (Puget and Stecker 1974) into the form

$$\epsilon_i(r) = \frac{2(1-r^2)}{h} \int_2^{r_m^2} d\eta (\eta-r^2)^{-1/2} \frac{d}{d\eta} (-I_i(\ell) \sec \ell) \quad (3)$$

where  $\eta \equiv \sin^2 \ell$ . This method has been shown to work well if confined to the longitude range within  $60^\circ$  of the galactic center, thus unfolding the inner Galaxy flux within the range  $0 \leq r \leq 0.86$ .

The IRAS 100 $\mu$ m fluxes were integrated over a range of  $\pm 1^\circ$  in galactic latitude around the midplane. The resultant distribution is shown in Fig. 5. To eliminate pointlike and small extended sources, thus separating out the underlying diffuse emission, an infimum filter was employed. This filter



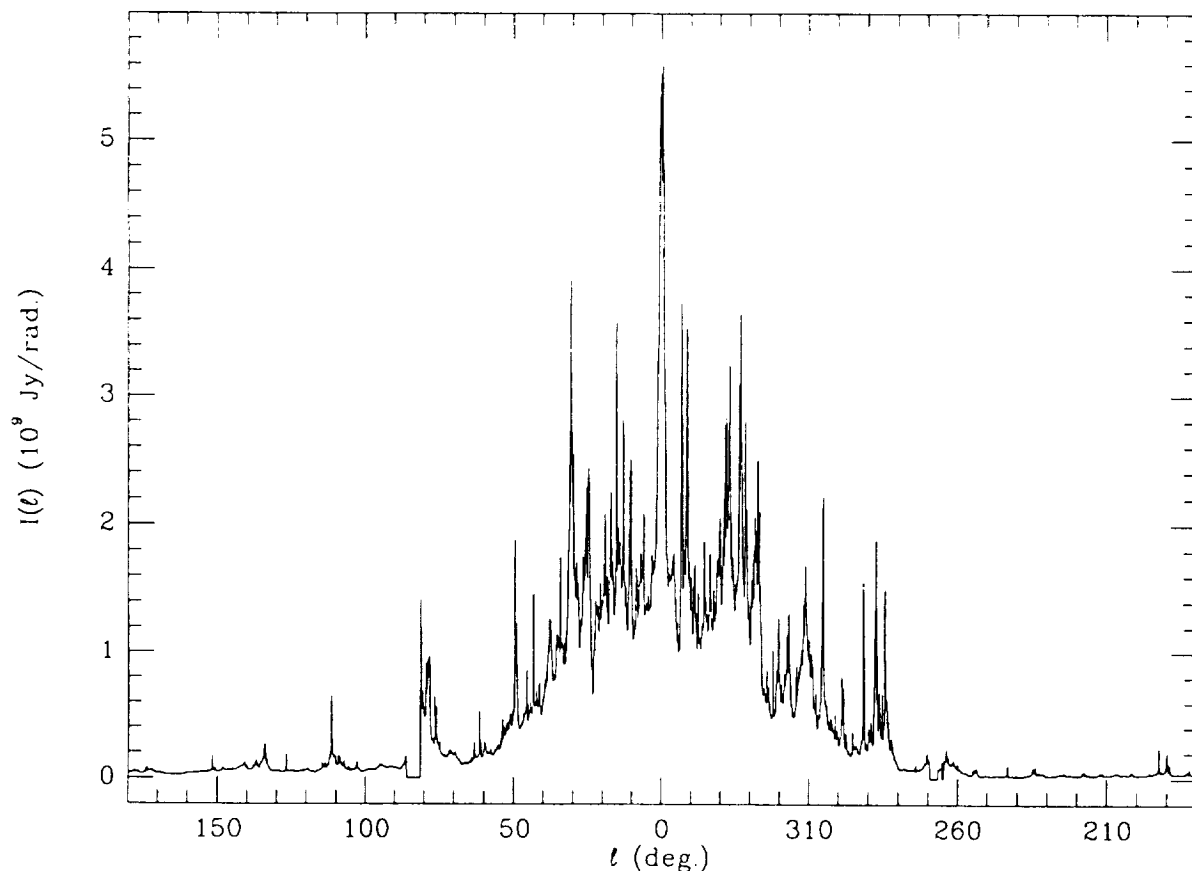


Figure 5. The observed 100  $\mu$ m IRAS flux longitude distribution from the galactic plane integrated over  $\pm 1^\circ$  in latitude.

chooses the greatest lower bound to the latitude integrated intensity in longitude intervals of  $1^\circ$ , cutting out features of less than  $1^\circ$  angular extent. We were then left with a few strong nearby far-infrared source which happen to be located at low galactic longitude such as M16, M17, W22, W33 and FIR 352.3. Because these sources are relatively close and strong, they were not removed with the automatic infimum filter method and had to be removed by subtraction and interpolation. Since they are at low longitudes and nearby, the effect of leaving them in would be to produce an artificial overestimate of the far-infrared emissivity inside of 4 kpc from the galactic center when the geometric unfolding algorithm was applied. After these sources were also removed, the longitude profile of the emission was regenerated by spline fitting the remaining diffuse flux values. The resulting distribution obtained is shown in Fig. 6. In order to give a more intelligible picture of the galactic large scale structure, a further averaging over  $4^\circ$  intervals in longitude was used before unfolding in order to obtain the radial distribution of the diffuse emissivity. We have checked our calculations by using the unfolded emissivity distributions and integrating them over the line-of-sight for various galactic longitudes as in eq. (2) to regenerate the FIR longitude distribution. The derived longitude profile faithfully reproduces the IRAS data profile, thereby demonstrating the accuracy of the unfolding technique.

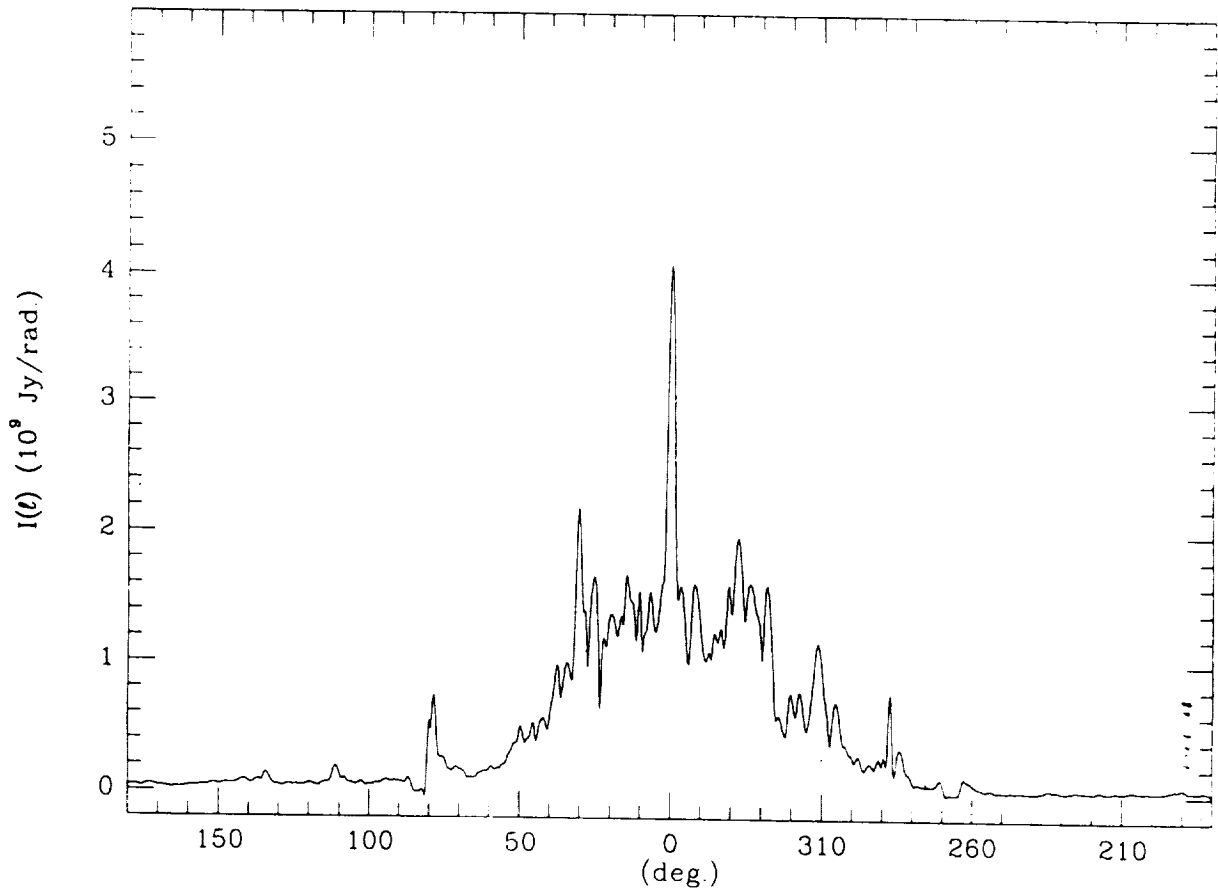


Figure 6. The IRAS flux distribution derived from Fig. 5 but with point sources removed.

A prima facie case for the close relationship between galactic  $\gamma$ -ray emission can be demonstrated by a direct comparison of their galactic longitude distributions. This has been done by the author (Stecker 1990) using the SAS-2 data, which are free of intrinsic detector background problems. A comparison of the diffuse IRAS emission profile (Fig. 6) with the 0.3-5 GeV COS-B longitude profile, obtained directly from the data tape, is shown in Fig. 7. We used the higher energy data because, although the photon count is lower, the angular resolution is better. We have offset the COS-B profile in Fig. 7, by subtracting a constant average background flux of  $3 \times 10^{-5} \text{ (cm}^2 \text{ s sr)}^{-1}$  in order to get a reasonable fit, something which was unnecessary in the case of the SAS-2 data. The author feels that owing to the uncertainty in the COS-B in-flight detector background, this additional "renormalization" may be allowable (Some may wish to consider our offset as merely suggestive or pedagogical.) At any rate, the future EGRET data should unambiguously determine the  $\gamma$ -ray flux in the anticenter direction.

The only obvious strong differences in the two profiles arise from the

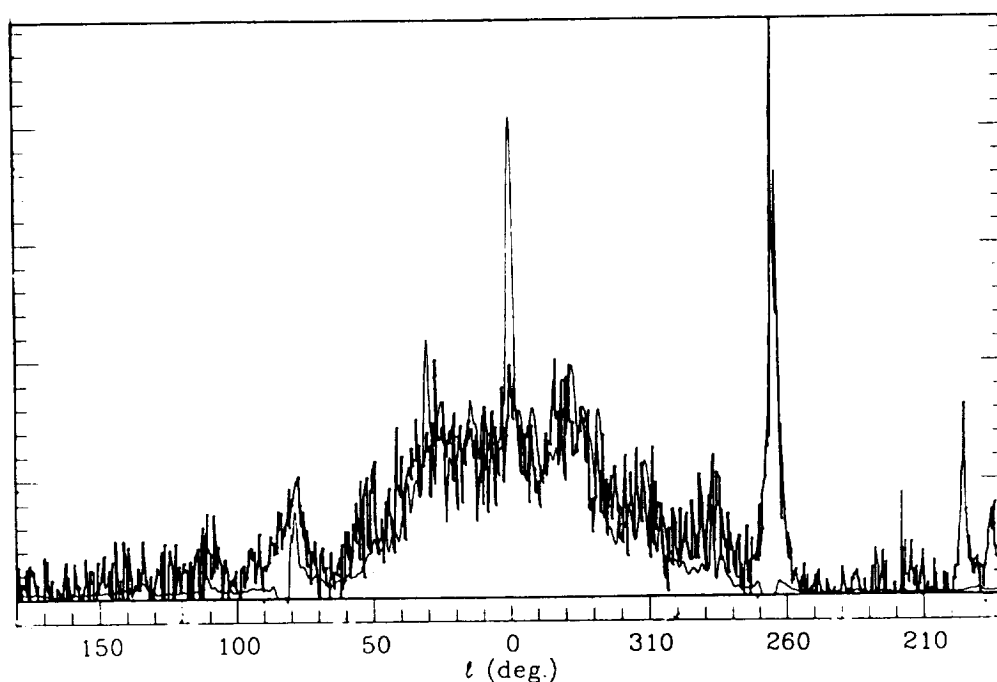


Fig. 7. A comparison of the point source subtracted IRAS longitude distribution shown in Fig 6 (light curve) with the COS-B 0.3-5 GeV galactic  $\gamma$ -ray flux profile averaged over  $\pm 10^\circ$  in latitude obtained from the final COS-B data tapes (heavy zig-zag line) with an additional offset subtraction of  $3 \times 10^{-5} \text{ (cm}^2 \text{ s sr)}^{-1}$  (see text).

known sources which are left in, *viz.*, the strong FIR source at the galactic center and the three intense  $\gamma$ -ray sources being the Crab and Geminga in the anticenter direction and the Vela pulsar at  $l \sim 270^\circ$ .

The galactic far-infrared radial emissivity distributions which we obtained from our unfolding using eq. (3) are shown in Figures 7 through 9 and compared with the radial distributions of other galactic components. Error bars are shown in the case of the  $\gamma$ -ray data which are a result of the statistics of the relatively few photons involved. Of course, in the case of the IRAS data, such statistical errors are negligibly small. As can be seen from Figure 8, the distribution of  $\gamma$ -ray emission, obtained by unfolding the SAS-2 and COS-B longitude data (HS), correlates well with the FIR emission on a galactic scale, supporting the thesis that the galactic  $\gamma$ -ray emission is associated with the most active regions of young star formation in the Galaxy (Stecker 1976). A further test of this hypothesis lies in a comparison of the distributions of FIR and CO emission. Figure 9 shows a comparison with the total CO cloud emission, whereas Figure 10 shows a comparison for the northern hemisphere with the distribution of warm clouds.

The correlation between our unfolded FIR distribution and the warm CO cloud distribution is remarkably striking, indicating that IRAS is most sensitive to the warmer molecular clouds. This is not surprising, since the  $100\mu\text{m}$  IRAS emission drops sharply for grain temperatures below 25 K. An important implicit result here is that the pure geometrical unfolding used here to treat the IRAS data does not give significant distortions from the distribution obtained from CO data which makes use of velocity information.

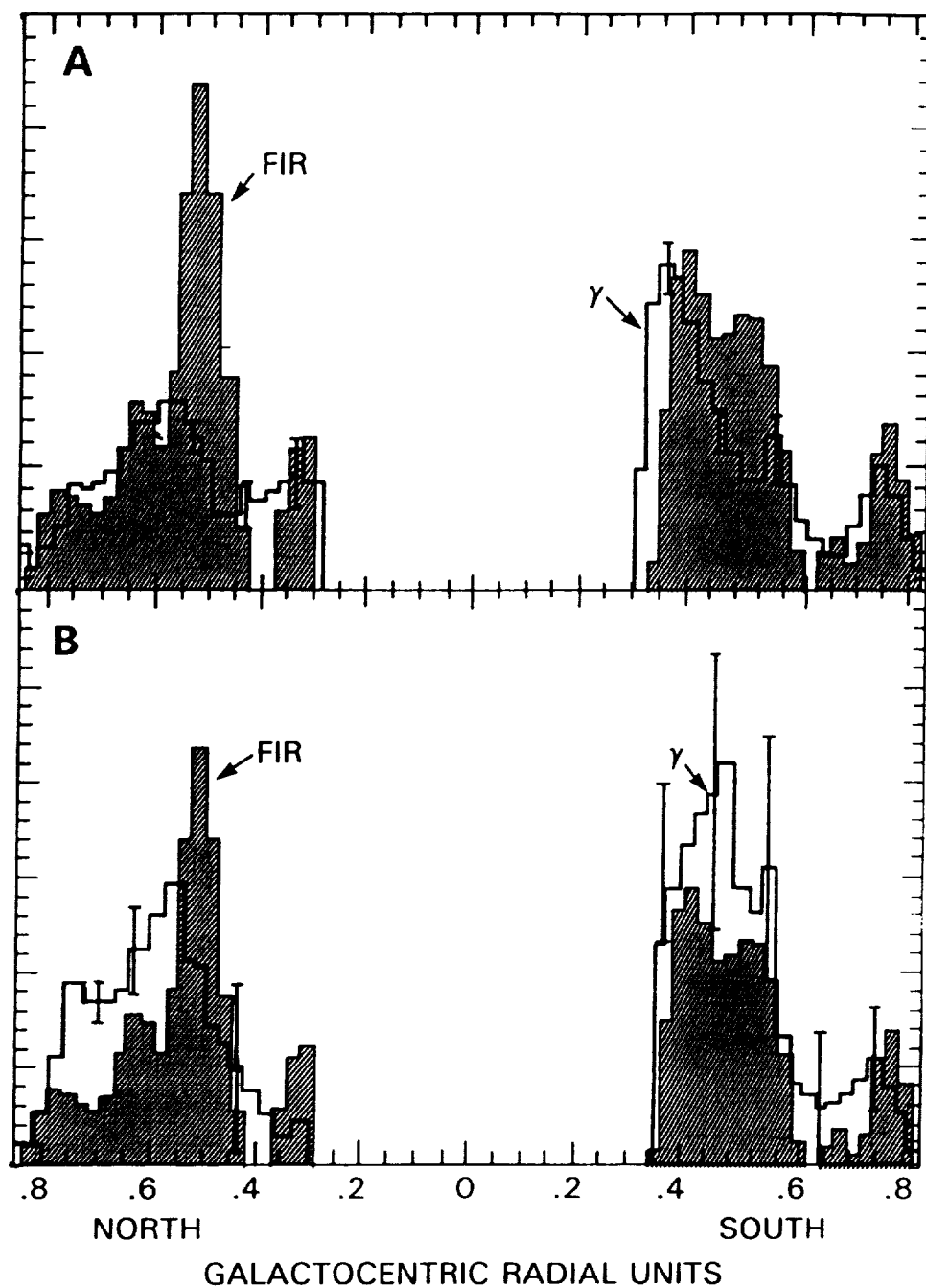


Fig. 8. (A) Relative  $\gamma$ -ray emissivity as a function of galactocentric distance derived from the COS-B data at energies greater than 100 MeV (Harding and Stecker 1985) as compared to the FIR emissivity distribution obtained here by a similar unfolding of the IRAS 100  $\mu$ m longitude map integrated over  $\pm 1^\circ$  in latitude. (B) A similar plot comparing the FIR distribution with the  $> 100$  MeV  $\gamma$ -ray distribution obtained from the SAS-2 data by Harding and Stecker (1985).

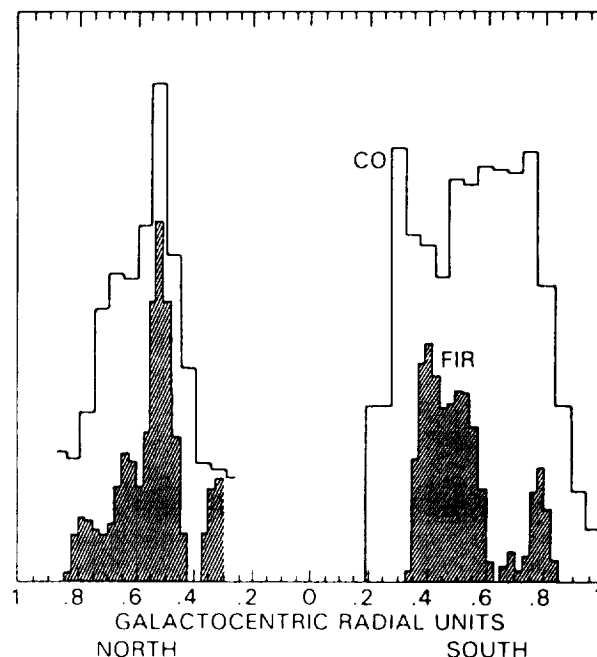


Fig. 9. A comparison of the total CO distribution in the southern galactic hemisphere at latitude  $0^\circ$  (Robinson, et al. 1984) and in the northern galactic hemisphere integrated over  $1^\circ$  (Scoville and Sanders 1986) with the FIR emissivity distribution (as in Fig. 8).

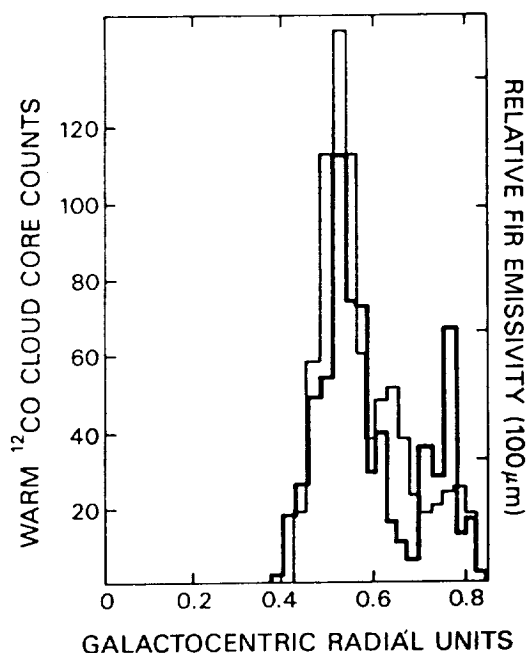


Fig. 10. A comparison of the warm CO cloud distribution in the northern hemisphere (Solomon, Sanders, and Rivolo 1985) (heavy histogram) with the FIR emissivity distribution from the northern hemisphere as in Figs. 8 and 9 (light histogram).

The overall FIR and warm CO emissivity distributions appear to be consistent with the concentration of these components to spiral arms as delineated by HII regions. However, the total CO distribution appears to be more diffused than the far-infrared emission. The overall picture which emerges appears to support the view that the total molecular cloud population is not confined only to spiral arms, but that the warm clouds, strongly heated by O and B stars, are associated with spiral arm structure.

Both the warm CO and FIR distributions show characteristic peaks in the north at radial units of  $\sim 0.5$  and  $\sim 0.75$  corresponding to the 5 kpc ring and Sagittarius arm respectively. There is a hint of a possible secondary peak in both distributions at  $\sim 0.6$ . One could speculate that this is an indication that two spiral arms may lie within the 5 kpc ring. Figure 10 also suggests that the FIR emissivity per cloud is higher in the 5 kpc ring than in the Sagittarius arm. The total CO and  $\gamma$ -ray distributions also correlate well in the northern region, but do not show detailed structure. In the case of the  $\gamma$ -rays, this may be due in part to the poorer angular resolution; there is some hint of a shoulder in the  $\gamma$ -ray distribution corresponding to the Sagittarius arm. In the south, one sees both the 5 kpc ring and peaks at  $\sim 0.8$  corresponding to the Crux arm in both the  $\gamma$ -ray and FIR distributions.

Our results, clearly showing the 5 kpc ring, are in general agreement with earlier balloon flight results of Caux, et al. (1984) and with the coarser unfolding of the IRAS data by Burton, et al. (1986) and Sodroski (1988), who also find evidence for strongly peaked emission originating in the 5 kpc ring. Of the 14 nearby Sa and Sb type spiral galaxies surveyed in CO emission, 5 have been found to have molecular cloud rings (Young 1987). Young and Scoville (1982) have noted a distinct correlation between the spatial distributions of blue-light emission and molecular clouds in Sc galaxies. For our Galaxy, Scoville and Good (1987) find that molecular clouds associated with HII regions are almost an order of magnitude brighter per unit cloud mass than clouds not associated with HII regions, the difference owing to the presence of O and B stars in the former. One must conclude that the large amount of far-infrared emission coming from the GGR strongly implies a large increase in the gas density and star formation rate there.

The fundamental result presented here is that a direct deconvolution of the far infrared luminosity distribution, independent of both the atomic and molecular gas observations, yields a radial distribution which clearly shows the molecular cloud ring at 4-8 kpc. This feature is clearly seen in all population I tracers e.g., CO, radio HII regions, pulsars and SN remnants, as well as  $\gamma$ -rays (Stecker 1976), but not in 21 cm HI surveys.

This result clearly links the molecular cloud distribution (rather than atomic) to the cycle of star formation and hence luminosity generation in the Galaxy. The picture of galactic activity borne out by  $\gamma$ -ray, CO and far-infrared surveys of the Galaxy delineates the cycle of activity in regions of active star formation. The OB associations condense out of cool dusty molecular clouds through gravitational collapse. The O and B stars ionize the gas around them to create HII regions and heat the dust in the surrounding clouds, causing them to reradiate in the far infrared band. At the end of their short life they explode into supernovae. Cosmic rays are produced

either in the shock waves generated by the supernova explosions or in the pulsars which they leave behind. Colliding with atomic nuclei primarily in molecular clouds, they produce  $\gamma$ -rays. The compound effect of cosmic rays and molecular clouds being enhanced in the 5 kpc ring leads to strong  $\gamma$ -ray emission there. In an analogous way, the compound effect of enhanced dust density and radiation from the massive young stars leads to strong far-infrared emission in the 5 kpc ring. Since the gas-to-dust ratio in the Galaxy appears to be relatively constant, and since the supernovae are from the massive stars, it is logical to expect a strong large scale correlation between FIR and  $\gamma$ -ray emission. It follows from all of this evidence that the region of the 5 kpc molecular ring is a place where the young objects in the Galaxy are most prolific (Stecker 1976).

It remains to be seen what EGRET, with its higher angular resolution and sensitivity and expectedly low intrinsic background, will show us about the morphology of the galactic plane in  $\gamma$ -rays. However, because of the close relationship between the FIR emission, given by the very high resolution IRAS survey, and the galactic  $\gamma$ -ray emission, a detailed comparison of morphologies will shed light on the distribution of galactic cosmic rays and their diffusion characteristics.

#### ACKNOWLEDGMENTS

I would like to thank A. Harding, D. Leisawitz, T. Sodroski and N. Scoville for discussions, N. Scoville for supplying the IRAS data tape and J. Skibo for numerical work on the IRAS data. I would also like to thank J. Mattox and P. Sreekumar for help with the COS-B data.

## REFERENCES

- Bronfman, L., Cohen, R. S., Alvarez, H., May, J., and Thaddeus, P., 1988, Ap. J. **324**, 248.
- Burton, W. B., 1976, Ann. Rev. Astron. Ap. **14**, 275.
- Burton, W. B., Duell, E. R., Walker, H. J., and Jongeneelen, A. A. W., 1986, in Light on Dark Matter (ed. F. P. Israel) Reidel, Dordrecht, p357.
- Caux, E., et al., 1984, Astron. Ap. **137**, 1.
- Clark, G. W., Kraushaar, W. L. and Garmire, G. P., 1968, Ap. J., **153**, L203.
- Clemens, D. P., Sanders, D. B., and Scoville, N. Z., 1988, Ap. J. **327**, 139.
- Dame, T. M., et al., 1987, Ap. J. **322**, 706.
- Dermer, C. D., 1986, Astron. Ap. **157**, 223.
- Fichtel, C. E., et al., 1975, Ap. J. **198**, 163.
- Fazio, G. G. and Stecker, F. W., 1976, Ap. J. **207**, L49.
- Harding, A. K. and Stecker, F. W., 1985, Ap. J. **291**, 471.
- Lockman, F. J., 1979, Astrophys. J. **232**, 761.
- Mayer, C. J., et al., 1987, Astron. Ap. **180**, 73.
- Mayer-Hasselwander, H. A., et al., 1982, Astron. Ap. **105**, 164.
- Myers, S. T. and Scoville, N. Z., 1987, Ap. J. **312**, L39.
- Puget, J. L. and Stecker, F. W. 1974, Ap. J., **191**, 323.
- Roberts, W. W., Jr., et al., 1975, Astrophys. J. **196**, 381.
- Robinson, B. J., et al., 1984, Ap. J. **283**, L31.
- Sanders, D. B., Solomon, P. M., and Scoville, N. Z., 1984, Ap. J., **276**, 182.
- Sanders, D. B., Clemens, D. P., Scoville, N. Z., and Solomon, P. M., 1986, Ap. J. Suppl. **60**, 1.
- Scoville, N. Z. and Good, J. C., 1987, in Star Formation in Galaxies NASA-CP 2466, (ed. C. J. Lonsdale Persson), p.3.
- Scoville, N. Z. and Sanders, D. B., 1986, in Interstellar Processes, ed. H. Thronson and D. Hollenbach (Dordrecht: Reidel), p. 21.
- Scoville, N. Z. and Solomon, P. M., 1975, Astrophys. J. **199**, L105.
- Solomon, P. M. and Mooney, T. J., 1988, in Galactic and Extragalactic Star Formation (eds. M. Fich and R. Pudritz) Reidel, Dordrecht, in press.
- Solomon, P. M. and Rivolo, A. R. 1987, in The Galaxy (ed. G. Gilmore and B. Carswell) Reidel, Dordrecht, p.105.
- Solomon, P. M. and Sage, L. J., 1988, preprint.
- Solomon, P. M., Sanders, D. B. and Rivolo, A. R., 1985, Ap.J. **292**, L19.
- Solomon, P. M. and Stecker, F. W., 1974, Proc. ESLAB Gamma-Ray Symposium, Frascati (ESRO SP-106), p. 253.
- Sodroski, T. J., 1988, unpublished.
- Stecker, F. W., 1969, Nature **222**, 865.
- Stecker, F. W., 1970, Astrophys. and Space Sci. **6**, 377.
- Stecker, F. W., 1971, Cosmic Gamma Rays (Baltimore: Mono Book Corp.).
- Stecker, F. W., 1975, Phys. Rev. Letters, **35**, 188.
- Stecker, F. W., 1976, Nature **260**, 412.
- Stecker, F. W., 1977, Ap. J., **212**, 60.
- Stecker, F. W., 1979, Astrophys J. **228**, 919.
- Stecker, F. W., 1981, Proc. Greenbank Workshop on The Phases of the Interstellar Medium (Greenbank, N.R.A.O.) ed. J. Dickey, p. 151.
- Stecker, F. W., 1989, in Cosmic Gamma Rays, Cosmic Neutrinos and Related Astrophysics ed. M. M. Shapiro and J. P. Wefel (Dordrecht: Kluwer Acad. Press), p. 85
- Stecker, F. W., 1990, to be published in a Festschrift for Maurice Shapiro, Univ. Chicago Press, in prep.



- Stecker, F. W., Harding, A. K., Skibo, J., Scoville, N. Z., and Good, J. C., 1989, submitted for publication.
- Stecker, F. W., and Jones, F. C. 1977, Ap. J., 217, 843.
- Stecker, F. W., Solomon, P. M., Scoville, N. Z., and Ryter, C. E., 1975, Ap. J., 201, 90.
- Strong, A. W., et al., 1987, in Proc. 20th Intl. Cosmic Ray Conf. (Moscow) 1, 125.
- Young, J. S., 1987, in Star Formation in Galaxies NASA CP-2466 (ed. C. J. Lonsdale Persson) p. 197.
- Young, J. S. and Scoville, N. Z. 1982, Astrophys. J., 260, L41.

## DISCUSSION

*Joe Taylor:*

Was your elimination of point sources from the IRAS map done before or after the integration over latitude? It seems to me it would be more effective if done before.

*Floyd Stecker:*

The elimination of point sources was performed after the integration over  $\pm 1^\circ$  in latitude. We estimate that performing the cut before integration (2 dimensionally) will not make a significant difference in our large-scale results, however, we can look at this more closely.

*Volker Schonfelder:*

I would like the COS-B team members to discuss the discrepancies in galactic longitude distributions from SAS-2 and COS-B.

*Hans Mayer - Hasselwander:*

The longitude distributions derived from both experiments are found to be in good agreement on a large scale (inner galaxy -outer galaxy). On a scale of several degrees in some places significant differences are found. These most likely are attributable to long term changes in the instruments sensitivities which probably in all cases could not be corrected in a perfect manner.

*Wim Hermsen:*

A comparison of the skymaps derived from the data in the final COS-B data base with SAS-2 skymaps showed that the distributions are fully consistent on a large scale (e.g. outer galaxy, inner galaxy intensity ratios). There remain small scale differences which in part might be real. Furthermore, there is no remaining background problem in the COS-B data.



## *Pulsars*

